Journal of Materials Chemistry A

Accepted Manuscript

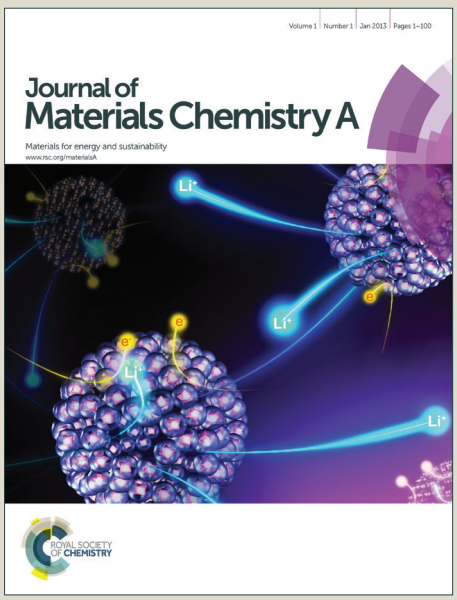

ROYAL SOCIETY OF CHEMISTRY

www.rsc.org/materialsA

Journal Name

RSCPublishing

COMMUNICATION

The Roles of Alkyl Halide Additives in Enhancing Perovskite Solar Cell Performance

Cite this: DOI: 10.1039/x0xx00000x

Chu-Chen Chueh,[a,+] Chien-Yi Liao,[a,+] Fan Zuo,[a] Spencer T. Williams,[a] Po-Wei Liang,[a] and Alex K.-Y. Jen[*a,b]

Received 00th January 2012,
Accepted 00th January 2012

DOI: 10.1039/x0xx00000x

www.rsc.org/

Alkyl halide additives have been investigated to elucidate their effects in enhancing perovskite solar cell performance. We found that the additives can participate in the perovskite formation via dissociated halides, suggesting that molecular structure of alkyl halide additives plays multiple roles in modulating the dynamics of perovskite crystal growth.

Processing of perovskite thin films on conducting polymers or metal oxide surfaces has been identified as one of the most critical steps in making high power conversion efficiency (PCE) devices with the rapid development of organometallic tri-halide perovskite ($CH_3NH_3PbX_3$, X= Cl^-, Br^-, or I^-) based solar cells. It has been demonstrated that the morphology and crystallinity of perovskite thin films can significantly affect their resultant photo-physical properties, such as light harvesting, exciton binding energy, and charge carrier mobility and lifetime.[1-2] Therefore, diverse processing techniques including physical vapor deposition,[3-4] one-step solution deposition,[5-9] vapor-assisted solution deposition,[10] and sequential solution deposition[11-18] have been exploited to control the quality of the formed thin films.

Since the first two-step solution process reported by Burschka *et al.* that can enhance the crystallinity of perovskite thin films,[11] the sequential solution processing techniques have become the prevailing methodology to achieve high-performance perovskite solar cells in dye-sensitized scaffolds (DSSCs) and planar heterojunction (PHJ) architectures.[11-18] For example, a vapor-assisted solution process has been developed by Yang *et al.* to obtain polycrystalline perovskite thin films with microscale grain sizes, leading to high PCE (>12 %) in inverted PHJ devices.[10] Very recently, the inter-diffusion between PbI_2 and methyl ammonium iodide (MAI) in a sequential deposition process has been employed by Huang *et al.* to fabricate high quality perovskite films on PEDOT:PSS to achieve very high PCE of >15 % in the conventional PHJ devices.[13] Moreover, the addition of methyl ammonium chloride (MACl) in a MAI solution (for the PbI_2 coated substrates) has been reported by Bein *et al.* that can improve photovoltaic performance of devices from 8.5% to ~15%.[14] This improvement is due to elongated photoexciton lifetime, increased band-edge light harvesting, and reduced device series resistance that can be achieved in mixed halide perovskites ($CH_3NH_3PbI_XCl_{3-X}$) compared to those derived from the tri-iodide perovskites ($CH_3NH_3PbI_3$). This validates the original findings reported by Snaith *et al.* in a one-step solution spin-coating.[2,5a] All these results show the impact of different processing techniques can affect the properties of perovskite thin films.

Compared to the flexibility in tuning sequential solution depositions to achieve optimum perovskite film growth, one-step solution deposition seems to be less adaptable due to limited variety of precursor compositions.[5-9] As mentioned earlier, the incorporation of Cl^- into the precursor solution by using $PbCl_2$ (namely a precursor solution consisting of 3MAI + $PbCl_2$ instead of MAI + PbI_2) greatly enhances crystallinity of the resulting perovskite thin films.[2,5] By adding chloride, it affects the pathway and kinetics of perovskite crystal growth and the quality of film formed. As a result, the mixed halide perovskites, $CH_3NH_3PbI_XCl_{3-X}$, possess greatly improved photo-physical properties compared to those derived from pure iodide-based perovskite.[2,5]

Another important benefit derived from prolonged crystallization process is the enhanced film coverage, especially for devices with planar interfaces. Achieving homogeneous crystal formation across a planar interface is quite challenging due to difficulty in controlling crystal nucleation, which is an event intimately associated with the crystallization kinetics.[5a,7-9,19-22] Thus, the inclusion of Cl^- has become the most ubiquitously applied strategy for improving film crystallinity and coverage in high performance PHJ solar cells fabricated by one-step solution process.[7-9,19]

In addition to Cl^- addition, solvent and precursor concentration can also affect the deposition dynamics via solvent-solute interactions, therefore, solvent engineering is another focal area that can be used to fine-tune one-step solution process.[6,23-25] Due to sensitive self-assembly of organo-lead halide perovskite in solution,

numerous solvent systems have been explored to optimize perovskite crystal formation. Recently, we have demonstrated that solvent additives can be incorporated into the precursor solution to effectively enhance the crystallinity and coverage of perovskite thin films on PEDOT substrates.[7a] The diiodo octane additive can modulate the rate of perovskite crystallization due to its ability to introduce specific solvent-solute interactions like ligation and chelation to alter the kinetics of crystallization. Since alkyl chain length and end-group of these halide additives may also play a role in affecting the dynamics of relevant solvent-solute interactions, we have further explored the feasibility of controlling intermolecular interactions by optimizing their molecular structures.

In this study, alkyl halides with different alkyl chain lengths and end-groups have been systematically investigated to elucidate their influence on the performance of perovskite solar cells, as shown in **Figure 1**. All the studied additives have resulted in clearly enhanced crystallization and substrate coverage in solution-processed perovskite thin films. As a result, PCE of devices made from these additive-enhanced perovskites increase from 9.8% (based on pristine perovskite) to as high as 13.1%. We have also found that these alkyl iodides might participate in the perovskite formation via dissociated C-X bond to generate extra X^- ions. These combined findings prove that alkyl halide additives can play multiple roles in modulating the dynamics of perovskite crystal growth.

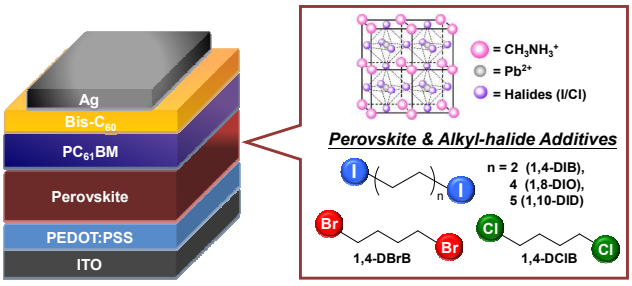

Figure 1. The configuration of PHJ device and the alkyl halide additives used in this study.

All the studied devices were fabricated using a low-temperature solution process (<150 °C) with a conventional p-i-n PHJ configuration of ITO/PEDOT:PSS (35-40 nm)/$CH_3NH_3PbI_{3-x}Cl_x$ (~350 nm)/$PC_{61}BM$ (~55 nm)/Bis-C_{60} (10 nm)/Ag (150 nm) (Fig. 1).[7] It is worthy to note that the thicknesses of $CH_3NH_3PbI_{3-x}Cl_x$ layers processed from precursor solutions containing different alkyl halides investigated were comparable as evidenced by the surface profilometer, where the thicknesses are all around 350 ± 50 nm. The mixed halide $CH_3NH_3PbI_{3-x}Cl_x$ was employed due to its ability of forming better crystal and thin film on PEDOT:PSS.[5a,7-9,19-22] It is important to mention that the recent argument over the residual Cl^- in the final $CH_3NH_3PbI_{3-x}Cl_x$ films has indicated no measureable quantity of Cl^- after thermal annealing.[26] The discussion of remaining Cl is beyond the scope of this work. Therefore, we still adopt $CH_3NH_3PbI_{3-x}Cl_x$ to denote the studied perovskite systems for convenience and clarity. Prior to the deposition of perovskite thin film, all the corresponding alkyl halides were added into the precursor solutions (3MAI + $PbCl_2$ + additives) with a 1 mol% blending ratio based on the amount of perovskite (denoted as 1% hereafter). In the studied device configuration, the Bis-C_{60} surfactant serves both as an efficient electron selective interlayer and as an energy realignment layer at the organic/metal interface.[27] This allows high work function metals to be used as the top electrode to achieve better environmental stability.[27] It is worth to note that the devices made from such PHJ architecture have been demonstrated to possess negligible hysteresis compared to those made from metal oxides (under a scan rate of 1 V/s in this study), which might result from the reduced density of traps across the PEDOT:PSS/perovskite interface.[7b,13,22,28-29] The detailed information for perovskite precursor solutions preparation, perovskite thin films deposition, and device fabrication is described in Supplementary Information.

The *J-V* and external quantum efficiency (EQE) curves of the best performing devices processed from precursor solutions containing 1% alkyl halides are summarized in **Figure 2a-b**. The relevant photovoltaic parameters such as open-circuit voltage (V_{OC}), short-circuit current density (J_{SC}), fill factor (FF), and PCE are listed in **Table 1** and their average values with standard deviation are presented in **Table S1**. Consistent with our previous finding,[7a] the device fabricated by adding 1% 1,8-diiodooctane (1,8-DIO) exhibited a much higher PCE_{MAX} of 11.62% with a V_{OC} of 0.92 V, a J_{SC} of 17.40 mA/cm^2, and a FF of 0.73 compared to that of the control device which only showed a PCE_{MAX} of ~9.8% and a relatively poor V_{OC} (0.88 V), J_{SC} (17.15 mA/cm^2), and FF (0.65). Previously, DIO was speculated to facilitate more homogenous perovskite nucleation across the surface of planar substrate and modulate the kinetics of its crystal growth. The diiodo end group of DIO may introduce additional solvent-solute interactions, like ligation or chelation during deposition and crystallization, which result in enhanced quality and coverage of perovskite thin films and performance of devices derived from them.[7a]

To understand the influence of alkyl chain length on device performance, different diiodo alkanes such as 1,4-diiodobutane (1,4-DIB), 1,10-diiododecane (1,10-DID), and 1,8-DIO were systematically studied. Encouragingly, the device made from the solution containing 1% 1,4-DIB showed a very promising PCE_{MAX} of 13.09% with a V_{OC} of 0.94 V, a J_{SC} of 18.47 mA/cm^2, and a FF of 0.75. Besides, the stratified device configuration (Fig. 1) of this champion device was confirmed by the cross-section SEM image (**Figure S1**). These results are even higher than the value of 1,8-DIO derived device. In contrast, the device made with 1% 1,10-DID showed much lower performance, which is only comparable to that of the control device (V_{OC}: 0.89 V, J_{SC}: 17.25 mA/cm^2, FF: 0.65, and PCE: 10%). These results show a clear trend of enhanced photovoltaic performance when the chain length of the diiodo based additives is decreased (**Table S2**). This indicates that the additive induced solvent-solute interactions become weakened when the length of the alkyl chain is increased. On one hand, the excessively long alkyl chains may create steric hindrance for chelation with Pb^{2+} which will induce higher configurational entropy loss during coordination.[7a,30] On the other hand, the poorer compatibility between longer non-polar alkyl chain and very polar DMF solvent might impede the efficiency of solvent-solute interactions. Consistent with these hypotheses, the solubility of $PbCl_2$ in the

mixed solvents (DMF/additives) decreases as the alkyl chain length increases from 1,4-DIB to 1,10-DID (**Figure S2**).

Afterward, different alkyl halides have also been investigated. Since different tri-halide perovskites have been reported in the literature ($CH_3NH_3PbX_3$, X= Cl^-, Br^-, or I^-), it suggests that these alkyl halides may interact differently in highly dynamic perovskite systems during film deposition and growth.[8,31] To understand the effect of end-group on device performance, two other additives, 1,4-dibromobutane (1,4-DBrB) and 1,4-dichlorobutane (1,4-DClB) were chosen to compare with control 1,4-DIB derived device. As shown in Fig. 2a and Table 1, devices processed from the solutions containing 1% 1,4-DBrB and 1,4-DClB also showed different degrees of PCE enhancement compared to that obtained from the control device. The device with 1% 1,4-DBrB exhibited a PCE_{MAX} of 12.88% which is similar to that obtained from adding 1% 1,4-DIB (with a V_{OC} of 0.94 V, a J_{SC} of 18.95 mA/cm^2, and a FF of 0.72). While the device with 1% 1,4-DClB showed a lower PCE_{MAX} of 11.76% with a V_{OC} of 0.92 V, a J_{SC} of 17.44 mA/cm2, and a FF of 0.73. The degree of PCE enhancement relative to the control device decreases from 1,4-DIB (34%) to 1,4-DClB (20%). This implies that the reactivity of end-group can also affect solvent-solute interactions to certain degree.

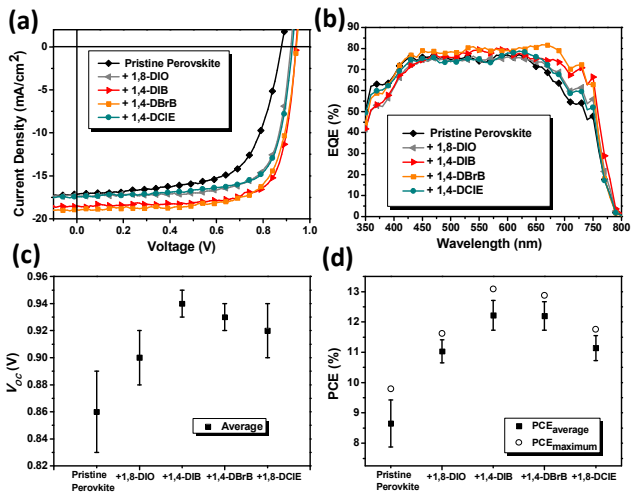

Figure 2. (a) *J-V* curves and (b) EQE spectra of the best studied PHJ solar cells under 100 mW cm^{-2} AM1.5 illumination. Statistics of (c) V_{OC} and (d) PCEs of the studied devices.

The curves of external quantum efficiency (EQE) in Fig. 2b confirm the accuracy of these devices, in which the difference between the integrated J_{sc} and the experimentally measured value is within 5%. As clearly shown, the peak EQE values of the top-performing 1,4-DIB and 1,4-DBrB based devices can reach over 80%. All the devices fabricated from precursor solutions containing 1% additives show higher EQE values (at incident wavelengths beyond 650 nm) and more reproducible device results (**Figure 2c** and **S3**), which affirms that better quality perovskite films were obtained as a result of additive inclusion.

The results of absorption spectra, X-ray diffraction (XRD) patterns, and scanning electron microscopy (SEM) shown in **Figure 3** clearly demonstrate that the addition of dihalides enhances crystallization of $CH_3NH_3PbI_{3-x}Cl_x$. The more intense band edge around 780 nm and increased light absorption across the entire absorption region are due to more uniform crystal growth and film formation in the additive-processed perovskite thin-films (**Figure 3a**). Such enhanced perovskite crystallization is also reflected in the XRD pattern (**Figure 3b**). All XRD patterns showed a tetragonal perovskite structure with a *I4cm* symmetry and a high phase purity.[7a,14,22,25] The higher intensity of diffraction peaks at 14.2°, 28.5°, and 43.2° (assigned to the (110), (220), and (330) crystal planes of $CH_3NH_3PbI_{3-x}Cl_x$) compared to those from the pristine perovskite is a clear evidence of enhanced perovskite crystallinity.[7a] These additive-processed thin films also have improved surface coverage (> 90%) as shown in the SEM images (**Figure 3c**). The simultaneously enhanced crystallization and surface coverage of these additive-assisted perovskite thin films contribute to the increased PCEs (Fig. S3). In addition, such difference in surface morphology and crystallinity also account for the observed variation in photovoltaic performance. The enhanced surface coverage and crystallization of perovskite films lead to reduced series resistance and increased shunt resistance, resulting in the improved J_{SC}, *FF*, and V_{OC} as observed (Table 1).

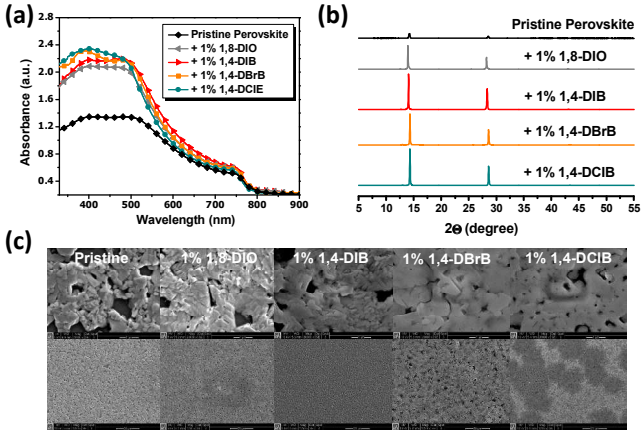

Figure 3. (a) UV-vis absorption spectra, (b) XRD spectra, and (c) SEM images of the solution-processed perovskite thin films with studied alkyl-halide additives. The scale bar for upper and lower SEM images is 1 and 20 μm, respectively.

Because the different electronegativity of each halogen atom, the C-X bond of each alkyl halide (X= Cl^-, Br^-, or I^-) is polarized differently, therefore, chemical reactivity of these alkyl halides also needs to be considered. Given that the bond strength of C-X decreases in the trend of C-Cl (78 kcal/mol) > C-Br (68 kcal/mol) > C-I (51 kcal/mol), the weaker C-X bond will facilitate easier C-X dissociation. This might lead to the generation of extra halide source to affect the coordination with Pb^{2+} during the perovskite formation.

In this regard, the 1,4-DIB with the weakest covalent C-X bond was mixed with a precursor solution only containing MACl + $PbCl_2$ (without any iodide source) to compare with the control perovskite thin film generated from the typical precursor composition (3MAI + $PbCl_2$). Note that the molar ratio between MACl, $PbCl_2$, and 1,4-DIB in the new formulation is 1:1:4, in which we have incorporated

Table 1. The summarized photovoltaic performance of the studied perovskite solar cells.[a]

	V_{OC} (V)[a]	J_{SC} (mA/cm^2)[a]	FF[a]	PCE (%)[a]
Pristine Perovskite	0.88	17.15	0.65	9.79
Perovskite + 1,8-DIO[b]	0.92	17.40	0.73	11.62
Perovskite + 1,4-DIB[b]	0.94	18.47	0.75	13.09
Perovskite + 1,4-DBrB[b]	0.94	18.95	0.72	12.88
Perovskite + 1,4-DClB[b]	0.92	17.44	0.73	11.76

[a] Best power conversion efficiencies (PCEs). The average values with standard deviation are described in the supporting information. [b] The amount of alkyl-halide additives is 1 mol% relative to perovskite in the precursor solution.

much higher concentration of 1,4-DIB than that is used for device fabrication in order to highlight the chemistry induced by alkyl iodides. Very interestingly, the characteristic peaks in XRD pattern (**Figure 4a**) and the absorption band-edge in UV spectra (**Figure 4b**) of the thin film processed from MACl + $PbCl_2$ + 1,4-DIB formula are almost identical to that of conventional $CH_3NH_3PbI_{3-x}Cl_x$ (processed from 3MAI + $PbCl_2$). In addition, both thin films look quite similar after thermal annealing at 90 °C for 2h, showing a dark brown color compared to the yellow color of the large bandgap $CH_3NH_3PbCl_3$ (Fig. 4a). All these results indicate that the thin-film processed form the new formula can result in the formation of $CH_3NH_3PbI_{3-x}Cl_x$. Since 1,4-DIB is the only source for iodide, this result obviously demonstrates that the C-I bond in 1,4-DIB was cleaved and the resulting iodide participated in the crystallization process of perovskite.

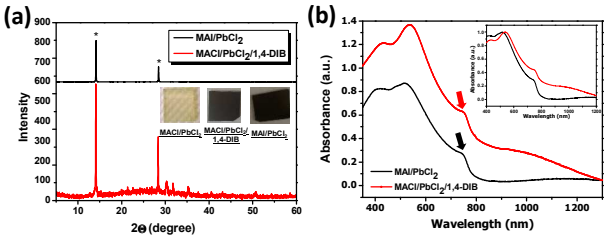

Figure 4. Comparison of (a) XRD and (b) UV-vis of the perovskite thin films processed from 3MAI+$PbCl_2$ (mole ratio: 3:1, 40 wt%) and MACl+$PbCl_2$+1,4-DIB (mole ratio: 1:1:4, 11.4 wt%). The insert in (a) are the real pictures of the perovskite thin films, processed from different precursor solutions, after thermal annealing at 90 °C.

Several possible underlying mechanisms might account for the observed C-I bond cleavage. As shown in **Scheme S1**, methylamine can be formed in the precursor solution or as a byproduct during degradation.[32] In this regard, the formed methylamine can serve as a nucleophile to react with 1,4-DIB to release iodide for taking part in the lattice formation of the perovskite. It is also possible that light can cleave the C-I bond to produce the same result as the abovementioned SN_2 reaction during the crystal formation.[33] Both reactions likely proceeded more rapidly during the stage of thermal annealing (90 °C) due to reduced Gibbs free energy. This discovery combined with our pervious finding[7a] enables us to conclude that the observed change of crystallization dynamics induced by alkyl halides should be the cooperative results of modulated solvent-solute interactions between alkyl halides and Pb^{2+} as well as the cleaved C-I bond during thermal annealing, as is illustrated in **Figure 5**.

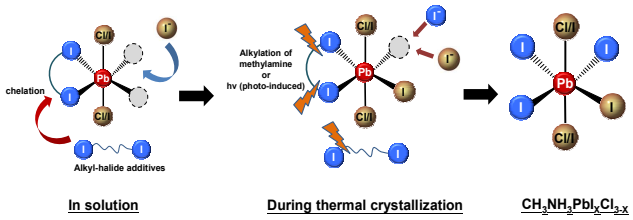

Figure 5. Illustration of the roles of alkyl-halide additives during perovskite crystallization as revealed by this work

Based on these observations, the bond strength of C-X (X= Cl^-, Br^-, or I^-) seems to have a profound effect on solvent-solute interactions. The grain size of perovskite thin films and their device performance are significantly dependent on how readily the C-X bond is cleaved. In addition, the boiling points of alkyl halides also affect their residual amounts in the deposited thin films, which can prolong the time to complete film evolution. These findings show the importance of understanding solution chemistry for manipulating the crystallization kinetics of organo-lead halide perovskites.

Conclusions

In summary, we have systematically investigated different chain lengths and end-groups of alkyl halide additives in affecting perovskite thin film evolution and device performance. All the studied additives enhance crystallization and surface coverage of solution-processed perovskite thin films and enable significantly enhanced PCE (from 9.8% in device made from a pristine perovskite to as high as 13.1% in additive-processed perovskites). Different degrees of PCE enhancements suggest that there are some correlations between the molecular structure of additives and device performance. We have also shown that C-X bond is susceptible to cleavage during the thermal annealing process, which frees halide ions to participate in perovskite formation. These findings show that alkyl halide additives serve multiple functions in modulating the dynamics of perovskite crystal formation. It opens up new perspective on perovskite preparation to continue the meteoric rise in efficiencies the field has seen thus far.

Acknowledgements

This work is supported by the Air Force Office of Scientific Research (FA9550-09-1-0426), the Office of Naval Research (N00014-11-1-0300), the Asian Office of Aerospace R&D (FA2386-11-1-4072). A. K.-Y. Jen thanks the Boeing-Johnson Foundation for financial support. C.Y. Liao thanks the financial support from the National Taiwan University. S. T. Williams thanks NSF GRFP (DGE-1256082) for financial support

Notes and references

[a] Department of Materials Science and Engineering, University of Washington, Seattle, WA 98195, USA. E-mail: ajen@u.washington.edu.
[b] Department of Chemistry, University of Washington, Seattle, WA 98195, USA.
[+] C.C.C and C.Y.L contributed equally to this work

† Electronic Supplementary Information (ESI) available: perovskite preparation, device fabrication and characterization. See DOI: 10.1039/c000000x/

1. C. C. Stoumpos, C. D. Malliakas, M. G. Kanatzidis, *Inorg. Chem.*, 2013, **52**, 9019.
2. S. D. Stranks, G. E. Eperon, G. Grancini, C. Menelaou, M. J. P. Alcocer, T. Leijtens, L. M. Herz, A. Petrozza, H. J. Snaith, *Science* 2013, **342**, 341.
3. M. Liu, M. B. Johnston, H. J. Snaith, *Nature* 2013, **501**, 395
4. C. W. Chen, H. W. Kang, S. Y. Hsiao, P. F. Yang, K. M. Chiang, H. W. Lin, *Adv. Mater.*, 2014, DOI: 10.1002/adma.201402461.
5. a) M. M. Lee, J. Teushcer, T. Miyasaka, T. N. Murakami, H. J. Snaith, *Science* 2012, **338**, 643; b) A. Abrusci, S. D. Stranks, P. Docampo, H. L. Yip, A. K. Y. Jen, H. J. Snaith, *Nano Lett.* 2013, **13**, 3124.
6. a) J. H. Heo, S. H. Im, J. H. Noh, T. N. Mandal, C. S. Lim, J. A. Chang, Y. H. Lee, H. J. Kim, A. Sarkar, M. K. Nazeeruddin, M. Gratzel, S. I. Seok, *Nature Photon.* 2013, **7**, 486; b) N. J. Jeon, H. G. Lee, Y. C. Kim, J. Seo, J. H. Noh, J. Lee, S. I. Seok, *J. Am. Chem. Soc.*, 2014, **136**, 7837; c) N. J. Jeon, J. H. Noh, Y. C. Kim, W. S. Yang, S. Ryu, S. I. Seok, *Nature Materials* 2014, **13**, 897.
7. a) P. W. Liang, C. Y. Liao, C. C. Chueh, F. Zuo, S. T. Williams, X. K. Xin, J. Lin, A. K. Y. Jen, *Adv. Mater.*, 2014, 26, 3748; b) P. W. Liang, C. C. Chueh, X. K. Xin, F. Zuo, S. T. Williams, C. Y. Liao, A. K. Y. Jen, *Adv. Energy Mater.*, 2014, DOI: 10.1002/aenm.201400960; c) F. Zuo, S. T. Williams, P. W. Liang, C. C. Chueh, C. Y. Liao, A. K. Y. Jen, *Adv. Mater.*, 2014, DOI: 10.1002/adma.201401641.
8. Y. Zhao, K. Zhu, *J. Phys. Chem. C.,* 2014, **118,** 9412.
9. H. P. Zhou, Q. Chen, G. Li, S. Luo, T. B. Song, H. S. Duan, Z. Hong, J. You, Y. Liu, Y. Yang, *Science* 2014, **345**, 542.
10. Q. Chen, H. Zhou, Z. Hong, S. Luo, H. S. Duan, H. H. Wang, Y. Liu, G. Li, Y. Yang, *J. Am. Chem. Soc.*, 2014, **136**, 622.
11. J. Burschka, N. Pellet, S. J. Moon, R. Humphry-Baker, P. Gao, M. K. Nazeeruddin, M. Gratzel, *Nature* 2013, **499**, 316.
12. D. Liu, T. L. Kelly, *Nature Photon.* 2013, **8**, 133.
13. a) Z. G. Xiao, C. Bi, Y. C. Shao, Q. F. Dong, Q. Wang, Y. B. Yuan, C. G. Wang, Y. L. Gao, J. S. Huang, *Energy Environ. Sci.*, 2014, **7**, 2619; b) Z. G. Xiao, Q. F. Dong, C. Bi, Y. C. Shao, Y. B. Yuan, J. S. Huang, *Adv. Mater.*, 2014, DOI: 10.1002/adma.201401685.
14. P. Docampo, F. Hanusch, S. D. Stranks, M. Doblinger, J. M. Feckl, M. Ehrensperger, N. K. Minar, M. B. Johnston, H. J. Snaith, T. Bein, *Adv. Energy Mater.*, 2014, DOI: 10.1002/aenm.201400355.
15. Ma, L. Zheng, Y. H. Chung, S. Chu, L. Xiao, Z. Chen, S. Wang, B. Qu, Q. Gong, Z. Wu, X. Hou, *Chem. Commun.*, 2014, DOI: 10.1039/C4CC01962H.
16. J. W. Lee, D. J. Seol, A. N. Cho, N. G. Park, *Adv. Mater.*, 2014, **26**, 4991.
17. C. H. Chiang, Z. L. Tseng, C. G. Wu, *J. Mater. Chem. A,* 2014,**2**, 15897.
18. Y. Z. Wu, A. Islam, X. D. Yang, C. J. Qin, J. Liu, K. Zhang, W. Q. Peng, L. Y. Han, *Energy Environ. Sci.* 2014, *7,* 2934.
19. J. M. Ball, M. M. Lee, A. Hey, H. Snaith, *Energy Environ. Sci.* 2013, *6,* 1739.
20. M. J. Carnie, C. Charbonneau, M. L. Davies, J. Troughton, T. M. Watson, K. Wojciechowski, H. Snaith, D. A. Worsley, *Chem. Commun.* 2013, **49**, 7893.
21. G. E. Eperon, V. M. Burlakov, P. Docampo, A. Goriely, H. J. Snaith, *Adv. Funct. Mater.* 2014, **24**, 151.
22. Q. Wang, Y. C. Shao, Q. F. Dong, Z. Q. Xiao, Y. B. Yuan, J. S. Huang, *Energy Environ. Sci.*, 2014, **7**, 2359.
23. J. Y. Jeng, Y. F. Chiang, M. H. Lee, S. R. Peng, T. F. Guo, P. Chen, T. C. Wen, *Adv. Mater.* 2013, **25**, 3727
24. B. Conings, L. Baeten, C. D. Dobbelaere, J. D'Haen, J. Manca, H. G. Boyen, *Adv. Mater.* 2014, **26**, 2041.
25. H. B. Kim, H. Choi, J. Jeong, S. Kim, B. Walker, S. Song, J. Y. Kim, *Nanoscale* 2014, **6**, 6679.
26. S. T. Williams, F. Zuo, C. C. Chueh, C. Y. Liao, P. W. Liang, A. K. Y. Jen, *ACS Nano,* 2014, DOI: 10.1021/nn5041922.
27. a) C. Z. Li, C. C. Chueh, H. L. Yip, K. M. O'Malley, W. C. Chen, A. K. Y. Jen, *J. Mater. Chem.*, 2012, **22**, 8574; b) C. C. Chueh, S. C. Chien, H. L. Yip, J. F. Salinas, C. Z. Li, K. S. Chen, F. C. Chen, W. C. Chen, A. K. Y. Jen, *Adv. Energy. Mater.* 2013, **3**, 417
28. J. Seo, S. Park, Y. C. Kim, N. J. Jeon, J. H. Joh, S. C. Yoon, S. I. Seok, *Energy Environ. Sci.*, 2014, DOI: 10.1039/C4EE01216J
29. H. J. Snaith, A. Abate, J. M. Ball, G. E. Eperon, T. Leijtens, N. K. Noel, S. D. Stranks, J. T. W. Wang, K. Wojciechowski, W. Zhang, *J. Phys. Chem. Lett.* 2014, **5**, 1511.
30. a) P. J. Albietz, J. B. P. Cleary, W. Paw, R. Eisenberg, *J. Am. Chem. Soc.* 2001, **123**, 12091; b) P. J. Albietz, J. B. P. Cleary, W. Paw, R. Eisenberg, *Inorg. Chem.* 2002, **41**, 2095.
31. a) J. H. Noh, S. H. Im, J. H. Heo, T. N. Mandal, S. I. Seok, *Nano Lett.* 2013, **13**, 1764; b) S. Ryu, J. H. Noh, N. J. Jeon, Y. C. Kim, W. S. Yang, J. Seo, S. I. Seok, *Energy Environ. Sci.*, 2014, **7**, 2614.
32. G. D. Niu, W. Z. Li, F. Q. Meng, L. D. Wang, H. P. Dong, Y. Qiu, *J. Mater. Chem. A* 2014, **2**, 705
33. P. J. Kropp, R. L. Adkins, *J. Am. Chem. Soc.* 1991, **113**, 2709

The Role of Alkyl Halide Additives in Enhancing Perovskite Solar Cell Performance

Chu-Chen Chueh, Chien-Yi Liao, Fan Zuo, Spencer T. Williams, Po-Wei Liang, and Alex K.-Y. Jen*

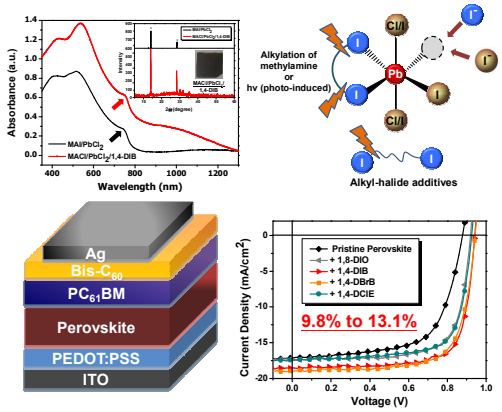

C-X bond of alky halide additives cleavages during thermal annealing, resulting in frees halide ions to participate in perovskite formation.